Journal of Science and Technology in Civil Engineering, HUCE, 2025, 19 (4): 58–68

A CATBOOST-BASED SURROGATE MODEL FOR FAST PREDICTION OF FREE VIBRATION RESPONSE IN TRI-DIRECTIONAL FUNCTIONALLY GRADED PLATES

Dieu T. T. Do[a,*], Son Thai[b,c]

[a]*Faculty of Management Information Systems, Ho Chi Minh University of Banking, 36 Ton That Dam street, Saigon ward, Ho Chi Minh City, Vietnam*
[b]*Faculty of Civil Engineering, Ho Chi Minh City University of Technology (HCMUT), 268 Ly Thuong Kiet street, Dien Hong ward, Ho Chi Minh city, Vietnam*
[c]*Vietnam National University Ho Chi Minh City (VNU-HCM), Linh Xuan ward, Ho Chi Minh city, Vietnam*

Article history:
Received 21/7/2025, Revised 06/10/2025, Accepted 16/10/2025

Abstract

Accurate numerical analysis of tri-directional functionally graded (3D-FGM) plates is computationally intensive, posing a major challenge for design optimization and reliability assessment. To overcome this, we propose an efficient surrogate model based on the CatBoost algorithm and benchmark its performance against a finely tuned Artificial Neural Network (ANN) for rapid prediction of free vibration responses. A high-fidelity dataset comprising 20000 samples was generated using a validated model that integrates Isogeometric Analysis (IGA) with Generalized Shear Deformation Theory (GSDT). Each sample includes eighteen input parameters (material control points) and three outputs: natural frequency, total ceramic volume fraction, and plate mass. The models were systematically evaluated by investigating the influence of hyperparameters and dataset size on prediction accuracy (measured by MSE and MAPE) and computational time. The results demonstrate that the optimized CatBoost model achieves nearly nine-fold lower test MSE and is over 10.8 times faster than the ANN. These findings highlight CatBoost as a highly accurate and efficient surrogate, enabling fast and reliable analysis of complex composite structures for future engineering applications.

Keywords: tri-directional functionally graded plates; CatBoost; artificial neural network; free vibration; machine learning; isogeometric analysis; surrogate model.

https://doi.org/10.31814/stce.huce2025-19(4)-05

1. Introduction

Functionally Graded Materials (FGMs) represent a sophisticated class of advanced composites, offering a superior alternative to conventional laminated materials. Unlike laminates with discrete interfaces prone to stress concentration and delamination, FGMs feature material properties that vary continuously and smoothly in one or more spatial directions. This gradual transition, typically between a ceramic phase providing high-temperature resistance and a metallic phase imparting fracture toughness, results in a composite with tailored, location-specific performance. Consequently, FGMs have been increasingly adopted in a wide range of demanding sectors, including aerospace engineering , nuclear plants, biomedical implants, and civil engineering [1–5]. While initial research focused on uni-directional (1D) FGMs, where properties vary only through the thickness, the need to withstand complex, multi-axial operational conditions has spurred the development of bi-directional (2D) and tri-directional (3D) FGMs. In 3D-FGM plates, the material composition is engineered to vary

*Corresponding author. *E-mail address:* dieudtt@hub.edu.vn (Do, D. T. T.)

along all three Cartesian coordinates, providing an unprecedented level of design freedom. A fundamental aspect of designing with these materials is the analysis of their dynamic behavior, particularly free vibration, which is critical for preventing catastrophic failure due to resonance.

The analytical complexity of 3D-FGM plates, however, makes closed-form solutions for vibration analysis intractable. Consequently, engineers rely on high-fidelity numerical methods like the Finite Element Method (FEM) and Isogeometric Analysis (IGA). While powerful, these methods are computationally expensive, as the need to capture continuous material variation requires fine mesh discretization and the solution of large systems of equations. This computational bottleneck becomes a critical barrier for essential engineering tasks that demand a large number of repeated analyses, such as structural optimization, reliability assessment, and the development of real-time "digital twins". To overcome this challenge, the engineering community has increasingly turned to surrogate models-data-driven, computationally inexpensive mathematical approximations of high-fidelity simulations. The core principle involves using a finite set of simulation data to train an approximation model that, once trained, can predict outputs for new inputs almost instantaneously. The application of machine learning (ML) has proven particularly effective for this purpose. Artificial Neural Networks (ANNs), particularly Multi-Layer Perceptrons (MLPs), are a well-established tool for surrogate modeling the complex mechanical behavior of FG structures. Indeed, numerous studies have successfully employed ANNs to predict a wide range of behaviors in FGM plates, including their dynamic responses, free vibration, and buckling characteristics [6–9].

More recently, ensemble learning methods, which combine multiple weak learners to create a single strong predictor, have gained prominence. Among these, gradient boosting decision tree (GBDT) algorithms have demonstrated exceptional performance on tabular data. Algorithms such as XGBoost and LightGBM have been successfully applied to analyze FG plates and other structural problems [10–16]. For example, Do et al. [11] utilized XGBoost for the transient analysis of FG plates, and Do [17] employed a suite of ensemble methods to predict the buckling behavior of tri-directional FG plates.

This paper focuses on CatBoost (Categorical Boosting), a state-of-the-art GBDT library that introduces key innovations to improve accuracy and reduce overfitting. Its primary advantages include Ordered Boosting, a permutation-driven training scheme that mitigates the target leakage problem, and the use of Symmetric (Oblivious) Trees. This tree structure acts as a powerful regularizer while also allowing for extremely fast predictions. The power and versatility of CatBoost have been demonstrated across a diverse range of recent engineering applications. In structural and materials engineering, it has been successfully used to predict the compressive strength of high-performance concrete [18] and to forecast construction delay risks [19]. Its capabilities also extend to geotechnical challenges, such as real-time rock mass classification in hard-rock tunnelling [20], and to energy systems, where it has been applied to predict residential heating consumption [21] and optimize electric vehicle battery state of charge estimation [22]. These diverse applications solidify its position at the forefront of applied machine learning.

Despite the successful application of ANNs and other boosting algorithms, a direct and rigorous comparison of a well-tuned CatBoost model against an optimized ANN for the specific problem of free vibration of 3D-FGM plates is currently absent from the literature. This study aims to fill this critical gap. The primary contributions of this work are the development of a high-performance CatBoost surrogate model for 3D-FGM plates and a rigorous, data-driven comparative analysis against a benchmark ANN. The models are holistically evaluated based on prediction accuracy (MSE and MAPE) and computational efficiency (training time), using a large-scale dataset of up to 20000 sam-

ples. This paper also generates valuable insights into the influence of dataset size and hyperparameter tuning on the performance of both modeling approaches for this class of complex structural dynamics problems.

2. Machine learning framework and Dataset

2.1. Problem formulation and Data generation

In this study, the dataset is generated from a high-fidelity numerical model grounded in two key theoretical concepts. The first is the use of tri-directional functionally graded materials (3D-FGM), which are advanced composites with properties varying continuously along all three Cartesian coordinates. This material variation is often described by the volume fraction of the ceramic constituent, V_c. For instance, a common approach is a power-law model:

$$V_c\left(x,y,z\right)=\left(\frac{x}{a}\right)^{k_x}\left(\frac{y}{b}\right)^{k_y}\left(\frac{1}{2}+\frac{z}{h}\right)^{k_z} \tag{1}$$

where k_x, k_y, k_z are the power-law indexes along the plate's dimensions a, b, h. The effective material properties, P, can then be estimated using schemes like the rule of mixture:

$$\mathrm{P}\left(\xi,\eta,\zeta\right)=\mathrm{P}_c V_c\left(\xi,\eta,\zeta\right)+\mathrm{P}_m V_m\left(\xi,\eta,\zeta\right) \tag{2}$$

The second concept is the Generalized Shear Deformation Theory (GSDT), an efficient higher-order plate theory used to analyze the mechanical responses. GSDT accurately captures shear deformation effects across the plate's thickness without requiring shear correction factors. The theory is characterized by its unique displacement field, where the in-plane displacements (u, v) for any point in the plate are defined as:

$$\begin{aligned} u\left(x,y,z,t\right)&=u_0\left(x,y,t\right)-zw_{0,x}\left(x,y,t\right)+f\left(z\right)\beta_x\left(x,y,t\right)\\ v\left(x,y,z,t\right)&=v_0\left(x,y,t\right)-zw_{0,y}\left(x,y,t\right)+f\left(z\right)\beta_y\left(x,y,t\right)\end{aligned} \tag{3}$$

here, u_0, v_0, w_0 are the mid-plane displacements, β_x, β_y are the rotations, and $f(z)$ is a shape function that defines the distribution of transverse shear strain through the thickness. In the referenced model, this shape function is given by:

$$f\left(z\right)=z-\frac{4z^3}{3h^2} \tag{4}$$

This theoretical framework provides the basis for the isogeometric analysis used to generate our training data.

The foundation of this study is a high-quality dataset generated from a numerical model of a tri-directional FGM plate. The model is based on a robust combination of Isogeometric Analysis (IGA) and a Generalized Shear Deformation Theory (GSDT), a methodology validated for its accuracy in our previous work [9].

Specifically, this study investigates the free vibration of a fully clamped (CCCC) tri-directional Al/Al_2O_3 square plate. The plate model under consideration is illustrated in Fig. 1. The plate has a length-to-thickness ratio (a/h) of 5. The material properties for the ceramic phase (Al_2O_3) are: $E_c = 380$ GPa, $v_c = 0.3$, and $\rho_c = 3960$ kg/m^3; and for the metal phase (Al): $E_m = 70$ GPa, $v_m = 0.3$, and $\rho_m = 2703$ kg/m^3. The effective material properties are estimated using the rule of mixture. A multi-mesh approach is employed, with a $3 \times 3 \times 1$ design mesh for material representation and a refined 15×15 cubic element analysis mesh to ensure solution accuracy.

The dataset is structured with 18 input variables (control points defining the material distribution) and 3 output variables: the first non-dimensional natural frequency, total ceramic volume fraction, and total mass. The non-dimensional frequency is calculated as $\bar{\omega} = \omega h \sqrt{\frac{\rho_m}{E_m}}$. To assess model scalability, three datasets were created with 5000, 10000, and 20000 data pairs. For all experiments, the data was randomly partitioned into a training set (80%) and a testing set (20%).

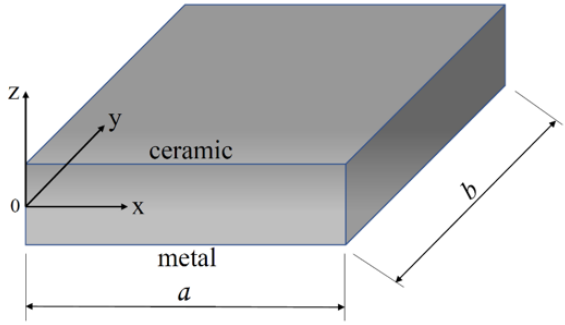

Figure 1. The functionally graded plate model

2.2. *Artificial neural network surrogate model*

The Artificial Neural Network (ANN) serves as the benchmark surrogate model in this study. Specifically, a Multi-Layer Perceptron (MLP), a class of feed-forward ANN, is used. The MLP is a powerful and flexible function approximator, capable of learning highly complex and nonlinear relationships between inputs and outputs, making it a standard choice for surrogate modeling in engineering.

The ANN architecture investigated is based on the configurations detailed in the provided data analysis. It consists of an input layer, one to three hidden layers, and an output layer. A systematic hyperparameter search is conducted by varying the number of hidden layers (one, two, or three) and the number of nodes (neurons) within each hidden layer (20, 50, or 100). The connections between nodes are governed by weights and biases, which are the parameters learned during the training process. The output of a neuron is determined by an activation function, which introduces nonlinearity into the network, allowing it to model complex patterns. Based on the experimental setup, the Softplus function is used as the activation function for the hidden layers.

The training process involves iteratively adjusting the network's weights to minimize a loss function that quantifies the difference between the model's predictions and the true target values. The Adam optimizer, an efficient and widely used gradient-based optimization algorithm, is employed for this purpose. The performance of the ANN is evaluated using two standard regression metrics:

- Mean Squared Error (MSE): This metric calculates the average of the squared differences between the predicted and actual values. It is defined as:

$$MSE = \frac{1}{n} \sum_{i=1}^{n} \left(Y_i - \hat{Y}_i \right)^2 \tag{5}$$

where n is the number of samples, Y_i is the actual value, and $\hat{Y}_i$ is the predicted value. MSE is particularly sensitive to large errors or outliers due to the squaring term.

- Mean Absolute Percentage Error (MAPE): This metric expresses the average absolute difference as a percentage of the actual values. It is defined as:

$$MAPE = \frac{100}{n} \sum_{i=1}^{n} \left| \frac{Y_i - \hat{Y}_i}{Y_i} \right| \tag{6}$$

MAPE provides an intuitive, relative measure of error and is less sensitive to the scale of the target variable. The use of both MSE and MAPE offers a more comprehensive and nuanced assessment of model performance than either metric alone.

2.3. CatBoost surrogate model

The primary focus of this investigation is the CatBoost algorithm, a state-of-the-art implementation of gradient boosting on decision trees (GBDT) [23]. Like other GBDT methods, CatBoost builds an ensemble of decision trees sequentially, where each new tree is trained to correct the errors made by the previous ones. However, CatBoost distinguishes itself through several novel architectural features that are hypothesized to give it a performance edge.

The key advantages of CatBoost, which form the basis for its evaluation in this study, are rooted in its sophisticated approach to model training and structure:

- Ordered boosting: to prevent the overfitting that can arise from target leakage, CatBoost employs a unique permutation-driven training process. For each sample in the training data, the model is updated using a separate model that was trained only on the samples that appeared earlier in a random permutation of the data. This clever technique ensures that the model learns from a "historical" perspective, preventing it from using information about the current sample's target to inform its own features, which leads to more robust and generalizable models.

- Symmetric (oblivious) trees: CatBoost grows decision trees in a balanced, symmetric fashion. At each level of the tree, the same feature and splitting criterion are used for all nodes. This structural constraint acts as a powerful regularizer, preventing the model from creating overly complex, deep branches that fit to noise in the training data. This not only improves the model's generalization but also results in a highly regular structure that can be evaluated with extreme speed, making CatBoost one of the fastest GBDT libraries for prediction.

- Computational efficiency: the algorithm is highly optimized for performance on both CPU and GPU architectures and has demonstrated excellent scalability on large datasets, a critical feature for modern machine learning applications.

The hyperparameter investigation for the CatBoost model is designed to explore the parameters that most directly control the bias-variance tradeoff. Based on the provided data analysis , the search space includes:

- Tree depth: The maximum depth of each decision tree, explored over the values {1, 2, 3, 4}. Deeper trees can capture more complex interactions but are more prone to overfitting.

- Learning_rate: A factor that shrinks the contribution of each tree, explored over the values {0.01, 0.05, 0.1, 0.2, 0.3, 0.4}. This range was chosen to cover a broad spectrum of learning behaviors, from slow and steady (low rates) for better generalization, to faster convergence (high rates). The inclusion of higher rates was validated by our results, as the optimal model for the largest dataset achieved its best performance with a learning_rate of 0.3.

To ensure a direct and fair comparison, the performance of the CatBoost model is evaluated using the same MSE and MAPE metrics as the ANN model.

3. Results and discussions

This section presents the study's main findings. First, the process of identifying the optimal settings (hyperparameters) for both the ANN and CatBoost models is presented. Subsequently, these optimized models are compared head-to-head to evaluate their performance based on prediction accuracy and computational cost.

All training processes were carried out using Python 3.7 on a laptop running Windows 11, 64-bit with an Intel® Core™ i7-8550U CPU @ 1.80 GHz 2.00 GHz, and 12.0 GB of RAM.

The performance of various ANN architectures was evaluated by systematically varying the number of hidden layers and the number of nodes per layer. The results, compiled from the experimental data, are detailed in Tables 1, 2, and 3, corresponding to the datasets with 5000, 10000, and 20000 data pairs, respectively. For each dataset, the optimal model was identified as the one providing the lowest Test MSE, indicating the best generalization performance.

Table 1. Performance of ANN architectures (Dataset size = 5000)

No. hidden layers		one-hidden layer			two-hidden layer			three-hidden layer		
No. nodes per layer		20	50	100	20	50	100	20	50	100
MSE	Training	1.41E-05	1.54E-05	2.92E-05	1.19E-05	1.10E-05	8.50E-06	1.31E-05	1.03E-05	1.97E-05
	Test	1.45E-05	1.56E-05	2.99E-05	1.16E-05	1.07E-05	8.14E-06	1.28E-05	1.01E-05	1.94E-05
MAPE (%)	Training	0.4580	0.5623	0.9139	0.4201	0.3695	0.3140	0.4641	0.4139	0.7245
	Test	0.4621	0.5622	0.9178	0.4170	0.3697	0.3084	0.4613	0.4125	0.7191
Time (sec)		145.49	150.99	156.24	162.80	173.47	179.52	176.70	183.63	211.81

As shown in Table 1 for the 5000-sample dataset: The optimal architecture is the two-hidden-layer model with 100 nodes each, which achieved a Test MSE of 8.14×10^{-6}. Although more complex models exist, this configuration provides the best balance between model capacity and generalization, avoiding the overfitting seen in overly complex structures on smaller data.

Table 2. Performance of ANN architectures (Dataset size = 10000)

No. hidden layers		one-hidden layer			two-hidden layer			three-hidden layer		
No. nodes per layer		20	50	100	20	50	100	20	50	100
MSE	Training	1.33E-05	1.61E-05	1.87E-05	1.09E-05	1.11E-05	6.63E-06	1.19E-05	9.58E-06	6.59E-06
	Test	1.50E-05	1.76E-05	2.02E-05	1.20E-05	1.19E-05	7.56E-06	1.35E-05	1.08E-05	7.25E-06
MAPE (%)	Training	0.4459	0.6299	0.6207	0.3696	0.3641	0.2610	0.4477	0.4251	0.3128
	Test	0.4685	0.6500	0.6368	0.3833	0.3721	0.2794	0.4697	0.4462	0.3240
Time (sec)		164.27	169.97	182.28	167.79	181.68	231.51	176.48	197.98	264.85

As presented in Table 2 for the 10000-sample dataset: The optimal model is the three-hidden-layer model with 100 nodes each, yielding a Test MSE of 7.25×10^{-6}. With more data available, a more complex architecture can be trained effectively, allowing it to capture more intricate patterns without significant overfitting, thus surpassing the performance of simpler models.

As detailed in Table 3 for the 20000-sample dataset: the optimal architecture remains the three-hidden-layer, 100-node model, which achieves the best overall performance with a Test MSE of 8.03×10^{-6}. While the test MSE on the 20000-sample dataset is slightly higher than that of the 10,000-sample dataset, this is attributed to dataset variance-a consequence of the stochastic nature of the data partitioning process. It is plausible that the random 20% split for the larger dataset resulted in a test set containing a higher proportion of outliers or more complex samples. The close proximity

of the training and test loss curves in Fig. 2 strongly suggests that the model generalizes well and is not suffering from overfitting.

Table 3. Performance of ANN architectures (Dataset size = 20000)

No. hidden layers		one-hidden layer			two-hidden layer			three-hidden layer		
No. nodes per layer		20	50	100	20	50	100	20	50	100
MSE	Training	1.33E-05	1.99E-05	1.51E-05	1.11E-05	1.66E-05	9.90E-06	1.07E-05	8.13E-06	7.90E-06
	Test	1.34E-05	2.02E-05	1.52E-05	1.10E-05	1.69E-05	1.03E-05	1.06E-05	8.33E-06	8.03E-06
MAPE (%)	Training	0.4095	0.6505	0.4754	0.3852	0.5772	0.3959	0.3551	0.3568	0.4067
	Test	0.4124	0.6554	0.4780	0.3850	0.5858	0.4031	0.3559	0.3618	0.4072
Time (sec)		167.23	178.54	185.13	169.01	210.20	250.62	191.61	240.99	294.50

A similar investigation was conducted for CatBoost, focusing on tree depth and learning_rate. The optimal model for each dataset was selected based on the lowest Test MSE, which also consistently corresponded to a low Test MAPE.

Table 4. Performance of CatBoost models (Dataset size = 5000)

depth	learning rate		0.01	0.05	0.1	0.2	0.3	0.4
1	MSE	Training	1.76E-04	7.96E-05	7.82E-05	8.04E-05	8.16E-05	8.14E-05
		Test	2.05E-04	9.74E-05	9.79E-05	1.01E-04	1.07E-04	1.14E-04
	MAPE (%)	Training	2.0356	1.1132	1.1080	1.1796	1.2062	1.2217
		Test	2.1968	1.2464	1.2426	1.3049	1.3637	1.4265
	Time (sec)		5.69	5.66	5.72	5.47	5.65	5.58
2	MSE	Training	5.08E-05	1.28E-05	8.19E-06	5.14E-06	3.86E-06	3.14E-06
		Test	6.90E-05	2.77E-05	2.52E-05	2.67E-05	2.68E-05	2.84E-05
	MAPE (%)	Training	1.0071	0.5077	0.4200	0.3392	0.2927	0.2656
		Test	1.1880	0.7201	0.6824	0.7267	0.7201	0.7417
	Time (sec)		7.96	8.12	7.98	7.89	7.91	7.8
3	MSE	Training	2.46E-05	5.19E-06	2.63E-06	1.10E-06	5.34E-07	2.70E-07
		Test	4.07E-05	1.97E-05	1.99E-05	2.46E-05	3.00E-05	3.19E-05
	MAPE (%)	Training	0.6911	0.3354	0.2432	0.1591	0.1100	0.0773
		Test	0.8893	0.6176	0.6214	0.6945	0.7666	0.8005
	Time (sec)		11.3	11.16	11.2	10.9	11.2	10.93
4	MSE	Training	1.39E-05	2.07E-06	6.78E-07	1.16E-07	2.44E-08	5.88E-09
		Test	3.07E-05	1.89E-05	2.10E-05	2.51E-05	3.25E-05	4.09E-05
	MAPE (%)	Training	0.5277	0.2138	0.1229	0.0499	0.0229	0.0112
		Test	0.7784	0.6123	0.6664	0.7366	0.8345	0.9262
	Time (sec)		15.45	16.18	16.08	15.58	15.61	16.13

In the case of the 5000-sample dataset (Table 4): The optimal model has a depth of 3 and a learning rate of 0.1, achieving a Test MSE of 1.99×10^{-5}. This configuration strikes a good balance, as deeper trees (depth 4) on this smaller dataset showed signs of overfitting with a slightly higher error.

Table 5. Performance of CatBoost models (Dataset size = 10000)

depth	learning rate		0.01	0.05	0.1	0.2	0.3	0.4
1	MSE	Training	1.76E-04	7.78E-05	7.75E-05	7.86E-05	8.05E-05	7.96E-05
		Test	1.92E-04	8.71E-05	8.79E-05	9.18E-05	9.53E-05	9.47E-05
	MAPE (%)	Training	2.0414	1.0743	1.0823	1.1294	1.1762	1.1830
		Test	2.1292	1.1512	1.1509	1.2311	1.2854	1.2987
	Time (sec)		7.74	7.45	8.04	7.72	7.66	8.34
2	MSE	Training	5.04E-05	1.25E-05	7.79E-06	5.02E-06	3.79E-06	2.97E-06
		Test	6.05E-05	1.87E-05	1.33E-05	1.09E-05	1.08E-05	1.07E-05
	MAPE (%)	Training	1.0042	0.4959	0.4070	0.3279	0.2838	0.2507
		Test	1.1109	0.5960	0.5121	0.4609	0.4471	0.4321
	Time (sec)		10.17	10.12	10.15	10.23	10.42	10.22
3	MSE	Training	2.44E-05	4.97E-06	2.71E-06	1.14E-06	6.12E-07	3.80E-07
		Test	3.20E-05	9.82E-06	7.62E-06	6.90E-06	6.81E-06	7.25E-06
	MAPE (%)	Training	0.6833	0.3230	0.2424	0.1547	0.1116	0.0861
		Test	0.7888	0.4390	0.3815	0.3271	0.2999	0.2888
	Time (sec)		13.87	14.03	13.65	13.54	14.38	13.89
4	MSE	Training	1.37E-05	2.08E-06	8.23E-07	1.97E-07	6.20E-08	2.16E-08
		Test	2.02E-05	6.52E-06	5.79E-06	5.96E-06	6.42E-06	8.13E-06
	MAPE (%)	Training	0.5148	0.2119	0.1298	0.0607	0.0332	0.0193
		Test	0.6288	0.3481	0.2978	0.2491	0.2215	0.2239
	Time (sec)		19.24	19.11	19.59	19.89	19.95	19.17

Results from the 10000-sample dataset (Table 5) indicate that the optimal configuration is a model with a depth of 4 and a learning rate of 0.1, which yields a Test MSE of 5.79×10^{-6}. The larger dataset allows a deeper tree to learn more effectively, resulting in a significant improvement in accuracy.

Table 6. Performance of CatBoost models (Dataset size = 20000)

depth	learning rate		0.01	0.05	0.1	0.2	0.3	0.4
1	MSE	Training	1.75E-04	7.83E-05	7.76E-05	7.72E-05	7.85E-05	7.86E-05
		Test	1.86E-04	8.20E-05	8.22E-05	8.26E-05	8.40E-05	8.70E-05
	MAPE (%)	Training	2.0379	1.0831	1.0941	1.1219	1.1515	1.1671
		Test	2.0916	1.1022	1.1281	1.1514	1.1894	1.2273
	Time (sec)		11.41	11.72	10.99	11.01	11.41	10.9
2	MSE	Training	5.10E-05	1.21E-05	7.61E-06	4.74E-06	3.35E-06	2.60E-06
		Test	5.61E-05	1.50E-05	1.02E-05	7.01E-06	5.58E-06	4.85E-06
	MAPE (%)	Training	1.0069	0.4865	0.3995	0.3170	0.2630	0.2304
		Test	1.0646	0.5351	0.4543	0.3777	0.3317	0.3038
	Time (sec)		14.44	14.29	14.23	14.84	14.36	15.13
3	MSE	Training	2.42E-05	4.78E-06	2.44E-06	1.00E-06	4.93E-07	3.06E-07
		Test	2.78E-05	6.86E-06	4.24E-06	2.34E-06	1.73E-06	1.47E-06
	MAPE (%)	Training	0.6827	0.3173	0.2291	0.1432	0.0985	0.0763
		Test	0.7335	0.3706	0.2906	0.2072	0.1572	0.1317
	Time (sec)		19.51	18.55	18.77	19.01	19.03	20.03

depth	learning rate		0.01	0.05	0.1	0.2	0.3	0.4
4	MSE	Training	1.35E-05	2.02E-06	7.20E-07	1.80E-07	5.98E-08	2.20E-08
		Test	1.64E-05	3.63E-06	1.78E-06	1.04E-06	9.01E-07	1.03E-06
	MAPE (%)	Training	0.5151	0.2065	0.1201	0.0570	0.0315	0.0185
		Test	0.5701	0.2668	0.1762	0.1056	0.0716	0.0562
	Time (sec)		27.25	28.19	28.19	27.56	27.04	28.44

Focusing on the 20000-sample dataset, Table 6 summarizes the performance where: The best performance is achieved with a depth of 4 and a learning rate of 0.3, resulting in an exceptionally low Test MSE of 9.01×10^{-7}. The combination of the largest dataset and a higher learning rate (enabled by more data) allows the model to converge to a much more accurate solution.

A direct comparison between the optimal ANN and CatBoost models at each data level reveals clear performance trends. In terms of prediction accuracy, while the ANN model performs better on the smallest dataset (5000 samples), CatBoost's performance scales much more effectively with data. At 10000 samples, CatBoost surpasses the ANN, and at 20000 samples, the optimal CatBoost model is significantly more accurate, with a Test MSE that is nearly 9 times lower than the best ANN model (9.01×10^{-7} vs. 8.03×10^{-6}). This demonstrates CatBoost's superior ability to leverage large, complex datasets without overfitting. Regarding computational eficiency, CatBoost holds a dramatic and consistent advantage in computational speed. For the largest dataset, the optimal CatBoost model trained in just 27.04 seconds, whereas the optimal ANN required 294.50 seconds. This makes CatBoost over 10.8 times faster, a critical advantage for any application requiring rapid model retraining or iterative analysis. While inference time is also a key metric, both the optimized ANN and CatBoost models perform single predictions almost instantaneously (on the order of milliseconds). Given this negligible difference for the intended engineering applications, the training time stands out as the more decisive measure of computational efficiency in this study.

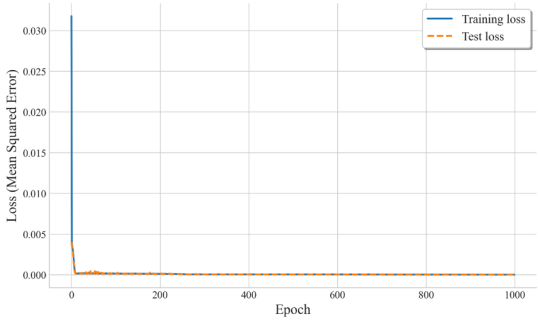

Figure 2. Convergence history of the optimal ANN model showing training and test loss over epochs

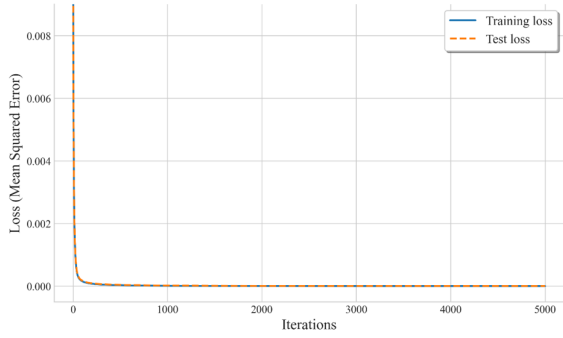

Figure 3. Convergence history of the optimal CatBoost model showing training and test MSE over iterations

The convergence histories of the optimal ANN and CatBoost models are visualized in Fig. 2 and Fig. 3, respectively. Both figures illustrate a stable and effective training process. For the ANN model (Fig. 2), the training and test loss curves decrease sharply in the initial epochs and then converge smoothly, remaining very close to each other. This proximity between the two curves indicates that the model generalizes well to new data and does not suffer from significant overfitting. Similarly, the CatBoost model (Fig. 3) also demonstrates rapid convergence, with the training and test MSE curves dropping quickly before plateauing at very low values. The small and stable gap between the

curves further confirms the model's robustness. When considered alongside the numerical results, it is evident that while both models are stable, the CatBoost model converges to a significantly lower final error state, visually reinforcing its superior accuracy.

For the problem of predicting the free vibration behavior of 3D-FGM plates, CatBoost emerges as the decisively superior surrogate model. It offers an exceptional combination of higher prediction accuracy, remarkable computational speed, and excellent scalability, making it a highly practical and robust choice for complex engineering analysis and future optimization tasks.

4. Conclusions

This paper presented the development and rigorous evaluation of surrogate models based on CatBoost and Artificial Neural Networks (ANN) for predicting the free vibration response of tri-directional functionally graded plates. The findings conclusively demonstrate that the CatBoost model is decisively superior to the benchmark ANN. The optimal CatBoost model achieved a nearly nine-fold reduction in prediction error (MSE) and was over 10.8 times faster to train on the largest dataset. Furthermore, the analysis highlighted CatBoost's excellent scalability, as its performance advantage became more pronounced with increasing dataset size. These results establish CatBoost as a powerful, fast, and reliable tool for structural engineers, enabling the acceleration of computationally intensive workflows such as design optimization and reliability analysis. Future work could focus on extending this methodology to more complex problems, including nonlinear analysis and the study of functionally graded shells.

Acknowledgements

We are grateful to Ho Chi Minh University of Banking for their support of this research.

References

[1] Rizov, V. (2025). Analysis of L-shaped functionally graded viscoelastic shafts with longitudinal crack under torsion. *Procedia Structural Integrity*, 68:139–145.

[2] Khan, M. D. A., Masanta, M. (2025). B4C-AISI 434 L steel functionally graded thin wall structures with variable B4C gradient strategies manufactured by TIG PBF-AAM method. *International Journal of Refractory Metals and Hard Materials*, 131:107210.

[3] Rajaeirad, M., Fakharifar, A., Posti, M. H. Z., Khorsandi, M., Watts, D. C., Elraggal, A., Ouldyerou, A., Merdji, A., Roy, S. (2024). Evaluating the effect of functionally graded materials on bone remodeling around dental implants. *Dental Materials*, 40(5):858–868.

[4] Akmal, M., Hussain, M. A., Ikram, H., Sattar, T., Jameel, S., Kim, J. Y., Khalid, F. A., Kim, J. W. (2016). In-vitro electrochemical and bioactivity evaluation of SS316L reinforced hydroxyapatite functionally graded materials fabricated for biomedical implants. *Ceramics International*, 42(3):3855–3863.

[5] Klecka, J., Cizek, J., Matejicek, J., Lukac, F., Vala, J. (2023). Thick functionally-graded W-316L composite coatings for nuclear fusion applications. *Nuclear Materials and Energy*, 34:101373.

[6] Shi, P., Wang, Z., Hoang, V. N. V., Zhao, W., Xie, H., Kiran, R., Yang, J. (2025). Analytical and neural network-based approaches for mechanical postbuckling analysis of simply-supported functionally graded graphene origami-enabled auxetic metamaterial plates. *Thin-Walled Structures*, 216:113606.

[7] Wojciechowski, M., Lefik, M., Boso, D. P. (2025). Differential evolution algorithm and artificial neural network surrogate model for functionally graded material homogenization and design. *Composite Structures*, 362:119041.

[8] Truong, T. T., Lee, S., Lee, J. (2020). An artificial neural network-differential evolution approach for optimization of bidirectional functionally graded beams. *Composite Structures*, 233:111517.

[9] Do, D. T. T., Nguyen-Xuan, H., Lee, J. (2020). Material optimization of tri-directional functionally graded plates by using deep neural network and isogeometric multimesh design approach. *Applied Mathematical Modelling*, 87:501–533.

[10] Nguyen, M.-C., Ha, M.-H., Nguyen, N.-T., Dinh, V.-T., Truong, V.-H. (2025). A robust XGBoost-based multi-objective optimization algorithm for nonlinear truss structures. *Journal of Science and Technology in Civil Engineering (JSTCE) - HUCE*, 19(1):Article 1.

[11] Do, D. T. T., Thai, S. (2023). Transient analysis of functionally graded plates using extreme gradient boosting. *Journal of Science and Technology in Civil Engineering (JSTCE) - HUCE*, 17(4):26–36.

[12] Tuan, V. V., Dinh, Q. T. (2025). Extreme gradient boosting model for forecasting slump and compressive strength of highperformance concrete. *Journal of Science and Technology in Civil Engineering (JSTCE) - HUCE*, 19(2):78–91.

[13] Qui, L. X. (2023). Damage identification of trusses using limited modal features and ensemble learning. *Journal of Science and Technology in Civil Engineering (JSTCE) - HUCE*, 17(2):9–20.

[14] Dieu, D. T. T., Yen, N. H. (2024). A light gradient boosting machine-based method for predicting the dynamic response of functionally graded plates. *Journal of Science and Technology*, 7(2).

[15] Truong, V.-H., Tangaramvong, S., Papazafeiropoulos, G. (2024). An efficient LightGBM-based differential evolution method for nonlinear inelastic truss optimization. *Expert Systems with Applications*, 237: 121530.

[16] Shehadeh, A., Alshboul, O., Al Mamlook, R. E., Hamedat, O. (2021). Machine learning models for predicting the residual value of heavy construction equipment: An evaluation of modified decision tree, LightGBM, and XGBoost regression. *Automation in Construction*, 129:103827.

[17] Do, D. T. T. (2024). Ensemble learning methods for the mechanical behavior prediction of tri-directional functionally graded plates. *Journal of Science and Technology in Civil Engineering (JSTCE) - HUCE*, 18 (4):98–108.

[18] Zhang, Y., Ren, W., Lei, J., Sun, L., Mi, Y., Chen, Y. (2024). Predicting the compressive strength of high-performance concrete via the DR-CatBoost model. *Case Studies in Construction Materials*, 21: e03990.

[19] Alsulamy, S. (2025). Predicting construction delay risks in Saudi Arabian projects: A comparative analysis of CatBoost, XGBoost, and LGBM. *Expert Systems with Applications*, 268:126268.

[20] Bo, Y., Liu, Q., Huang, X., Pan, Y. (2022). Real-time hard-rock tunnel prediction model for rock mass classification using CatBoost integrated with Sequential Model-Based Optimization. *Tunnelling and Underground Space Technology*, 124:104448.

[21] Dasi, H., Ying, Z., Yang, B. (2023). Predicting the consumed heating energy at residential buildings using a combination of categorical boosting (CatBoost) and Meta heuristics algorithms. *Journal of Building Engineering*, 71:106584.

[22] Sulaiman, M. H., Mustaffa, Z., Samsudin, A. S., Mohamed, A. I., Saari, M. M. (2025). Electric vehicle battery state of charge estimation using metaheuristic-optimized CatBoost algorithms. *Franklin Open*, 11:100293.

[23] Prokhorenkova, L., Gusev, G., Vorobev, A., Dorogush, A. V., Gulin, A. (2017). CatBoost: unbiased boosting with categorical features. *arXiv*.